Indian Journal of Biochemistry & Biophysics
Vol. 56, April 2019, pp. 105-116

Expression, purification and characterization of a biologically active and thermally stable human lysyl oxidase

Renganathan Bhuvanasundar[1,2], Nareshkumar Nagaraj Ragavachetty[1,3], Naveen Kumar Singh[2], Karunakaran Coral[1], Perinkulam Ravi Deepa[2] & Konerirajapuram Natarajan Sulochana[1]*

[1]Department of Biochemistry and Cell Biology, Vision Research Foundation, Sankara Nethralaya, Chennai -600 006, Tamil Nadu, India

[2]Department of Biological Sciences, Birla Institute of Technology and Science, Pilani -333 031, Rajasthan, India

[3]School of Chemical and Biotechnology, Sastra University, Thanjavur -613 401, Tamil Nadu, India

Received 28 December 2017; *revised 12 September 2018*

Lysyl oxidase (LOX), a promising therapeutic target for the progression of cancer and fibrosis, has not been well characterized yet. A major difficulty faced in LOX characterization is its lack of solubility in common buffers. In this study, mature LOX (mLOX) was cloned, purified and its purity was ascertained by mass spectroscopy. Through screening various buffers, 0.2 M glycine-NaOH buffer with 10% glycerol pH 8.0 was identified to maintain mLOX in its soluble state. About 67% of the refolded mLOX was found to be in copper bound state after His-tag removal. Catalytic properties K_m and k_{cat} were found to be 3.72×10^{-4} M and $7.29 \times 10^{3} s^{-1}$. In addition, collagen cross-linking in ARPE-19 cells was augmented on exposure to mLOX, endorsing its biological activity. Circular Dichroism revealed that mLOX comprises 8.43% of α-helix and 22% of β-strand and it was thermally stable up to 90°C. Disulfide linkage imparts the structural stability in LOX which was experimentally ascertained with intrinsic and extrinsic fluorescence studies.

Keywords: Enzyme kinetics, Recombinant mLOX, Spectroscopy and structure stability

LOX belongs to the copper-dependent amine oxidase family (EC number, 1.4.3.13) and has copper and lysine tyrosyl quinine (LTQ) as its cofactors. LOX pro-enzyme with a molecular weight of 50 kDa is secreted extracellular, where it is proteolytically cleaved by bone morphogenetic protein-1 into a catalytically active mature LOX of 32 kDa and a propeptide of 18 kDa[1]. LOX enzyme is responsible for the maturation of elastin and collagen by converting peptidyl lysine of the monomers into allysine and hence it is crucial for the formation of extracellular matrix (ECM)[2]. LOX, being a key player in the formation and preparation of ECM, its expression and activity are altered in ECM related diseases[3]. In addition to the role in cross-linking, LOX is also implicated in the progression of cancer. Its role in cancer has been validated in cell migration[4] and in tumour metastasis[5]. Expression of LOX enhances epithelial-to-mesenchymal transition (EMT) in cancerous condition by down regulating the cell adhesion molecule E-cadherin[6]. LOX enhance the tumour endothelial migration and angiogenesis *via* Akt pathway under the stimulation of VEGF/hypoxia[7,8]. Though mature LOX function as pro-angiogenic, N-terminal region of LOX is designated as pro-peptide and is known for its anti-angiogenic function[9,10]. From our group, we have shown the over expression of LOX pro-peptide in the endothelial cell inhibits angiogenesis[11]. Nevertheless, LOX is identified as a prognostic factor[12] and also a biomarker[13] in several cancerous conditions. Apart from cancer, aberrant expression of LOX has been reported as a diagnostic marker in fibrosis where the inhibition of its activity combats the fibrotic condition[14,15]. It has also been hypothesized that inhibition of LOX activity may be a possible way to reduce the stiffening of the trabecular meshwork in glaucoma[16,17]. Inhibiting the expression of LOX with βAPN, a known inhibitor for LOX, is shown to reduce the disease pathogenesis. However, lack of specificity of βAPN makes it a poor drug. Although the

*Correspondence:
Phone: +91-9791141159 (Mob)
E-mail: suloravi@gmail.com; drkns@snmail.org

Abbreviations: ANSA, 8-Anilino-1-napthalenesulfonic acid; DAP, 1,5-Diaminopentane; DTT, Dithiothreitol; Hcys, Homocysteine; LOX, Lysyl oxidase; mLOX, Mature Lysyloxidase; PLGS, Protein lynx global software; βAPN, β-aminopropionitrile

importance of targeting LOX in cancer[3] and other diseases like fibrosis[18], glaucoma[19] andcardiovascular diseases[20] has been well discussed, effective drugs are not available.

Conventional drug development for LOX is not possible because of the lack of its crystal structure. Further, studies on the structure of LOX and its stability are also limited. In aqueous buffers, LOX exhibits low solubility and aggregation, which remains an obstacle in its structural and functional characterization. In our previous study, we have reported LOX model using *ab initio* modelling with proper copper geometry by *in silico* approach[21]. Here, we endeavour to characterize the LOX enzyme by *in vitro* approach.

In this study, recombinant human mature LOX (mLOX) was purified and characterized. Recombinant mLOX was refolded into biological active enzyme in aqueous buffer devoid of urea. Biochemical properties such as optimal substrate concentration, pH and enzyme kinetics were identified and biological activity was substantiated with cell culture experiments. Thermal stability and secondary structure of mLOX were studied using CD spectra, intrinsic and extrinsic protein fluorescence experiments.

Materials and Methods

Construction, expression and purification of pQE-30Xa+mLOX expression plasmid

Human mLOX was cloned into pQE-30Xa vector between the *Stu* I and *Hind* III sites, as described in our previous report[22]. In brief, the mLOX gene was amplified from Human Umbilical Vein Endothelial Cells (HUVECs) cDNA (template) using the gene-specific primers *Stu* I 5′GGTATCGAGGGAAGGCC TGACGACCCTTACAACCCC3′ and *Hind* III 5′TCAGCTAATTAAGCTTCTAATACGGTGAAAT TGT3′. Using an infusion enzyme kit (Cat # 638909, Takara, Clontech, USA), pQE-30Xa+mLOX expression vector was constructed from the linearized vector and amplified mLOX DNA by following the manufacturer's protocol. pQE-30Xa+mLOX encodes the mLOX with six histidine residues (His tag) at the N-terminal linked through factor Xa cleavage site. Recombinant mLOX was expressed in M15 (pREP4) strain of *E. coli* from the transformed plasmid pQE-30Xa+mLOX. Transformed colonies were grown in Luria-Bertani broth containing 0.1 µg/mL of ampicillin and 0.025 µg/mL of kanamycin at 37°C. The culture at mid-log phase (absorbance unit 0.5-0.7 at 600 nm) was induced with 1 mM isopropyl-β-D-thiogalactopyranoside (IPTG) for expression of mLOX and was cultured for 4 h at 30°C. *E. coli* cells were pelleted down by centrifugation and re-suspended in lysis buffer (50 mM sodium dihydrogen phosphate, 300 mM sodium chloride, 8 M urea and protease inhibitor cocktail at a concentration of 1 mg/mL, pH 8.0). Suspension was incubated for 30 min at 4°C and the whole cell including inclusion bodies was lysed by sonication. Then the lysate was centrifuged at 12857 g for 30 min at 4°C and purification was carried out with the supernatant. The clarified supernatant was passed through the Ni-NTA affinity column equilibrated with lysis buffer. Non-specifically bound proteins were removed by stringent washing with 30 mM imidazole in lysis buffer and then His-tagged mLOX protein was eluted with lysis buffer containing 250 mM imidazole. The purity of the recombinant protein was confirmed by SDS-PAGE, western blot (LOX antibody, Cat # SC-32409, Santa Cruz Biotechnology and His tag antibody, Cat # 2365, Cell Signaling Technology,) and mass spectroscopy (MS). Protein estimation was done by using Pierce Coomassie plus protein assay kit (Bradford) (Cat # 23236, Thermo Fisher Scientific).

Mass spectroscopy (MS) analysis

Recombinant mLOX (1 µg) was suspended in 50 µL of 50 mM ammonium bicarbonate buffer, pH 9.0. Disulfide bonds were reduced using dithiothreitol (DTT) with the final concentration of 10 mM (60°C for 15 min) and alkylated with iodoacetic acid with the final concentration of 20 mM RT for 30 min. Trypsin 50 ng (Sigma proteomics grade, Cat # T6567) was added to the sample and digested for overnight at 37°C; digestion was stopped by adding 1 µL of 1% formic acid. Then excess salts were removed by Oasis HLB cartridge (Cat # WAT094225, Waters Corporation, USA) following manufacturer's protocol. Digested peptides were separated in nano UPLC and analysed with hybrid mass spectrometry (Xevo G2S QT of mass spectrometry coupled with Acuity nano LC, Waters, USA). The detected peptides were matched against UniProt human protein database using Protein Lynx Global Software (PLGS, version 2.5.3, Waters, USA) and identified the protein.

Screening for the buffer to maintain mLOX in solution

Optimum solubility screening is a systemic way to determine the solubility of a protein.A known amount

of the protein of interest will be re-suspended in various buffers with chemical additives and solubility will be checked by protein estimation after high-speed centrifugation in supernatant and pellet[23]. For crystallization studies, this approach is being followed to identify optimal buffer for protein solubility and stability. This approach was employed to identify buffer that would solubilize recombinant mLOX. Screened the following buffers: 10 mM dipotassium hydrogen phosphate buffer, 0.2 M HEPES-NaOH buffer, 0.2 M Tris-HCl buffer, 0.2 M borate buffer, 0.2 M arginine-NaOH, 0.2 M glycine-NaOH buffer over the pH range of 6-9. Glycerol, a co-solvent known to increase the protein stability, was added to the buffers up to a final concentration of 10%. In brief, purified mLOX protein was suspended in equal volume of above–tested buffers to the final concentration of 50 µg/150 µL and incubated at RT for 30 min. The solubility was checked by visible aggregation and further centrifuged at 10000 g for 10 min to identify any aggregation. Further, protein estimations were done in both the pellet and the supernatant.

Refolding of mLOX

Step-wise reduction in the denaturant concentration was implemented to refold mLOX. The rate of protein folding to its native structure increase by a step-wise reduction in the denaturant concentration[24]. Recombinant mLOX was refolded by a stepwise reduction in urea concentration. Purified mLOX was suspended and dialyzed against the identified buffer for 8 h using 3 kDa semi-permeable membrane and urea concentration was varied from eight molar to zero molar (in steps of 1 M difference/step). After refolding, His tag was removed from the mLOXusing factor Xa endoprotease (Cat # 33223, Qiagen, Hilden, Germany) in the presence of 1 mM calcium chloride reconstituted in the glycine-NaOH buffer at the pH of 8.0 at 37°C for overnight. After digestion, factor Xa protease was removed using factor Xa removal resin (Cat # 33213, Qiagen) following the manufacturer's protocol. Subsequently, undigested His tag protein was captured using Ni-NTA affinity column, while His tag free mLOX was collected as unbound protein. Complete removal of His tag was confirmed by western blot using His tag specific antibody.

Incorporation and estimation of copper in recombinant mLOX

His tag free mLOX was dialyzed against a glycine-NaOH buffer with copper (Cu) (2:1, Cu:protein concentration) for 4 h. Then free/unbound Cu was removed by dialysis against glycine-NaOH buffer free of Cu for 16 h. Cu bound to the recombinant mLOX was estimated by atomic absorption spectroscopy (A Analyst 7000, Perkin, USA). The instrument was calibrated with 0.2% nitric acid and background values for solvents (Milli-Q water and buffer) were determined and taken into account during calculation. Absorption of the known concentrations (2.5, 5, 7.5 and 10 µg/mL) of elemental copper was used as standards. mLOX (100 µg/100 µL) was reconstituted to 1 mL using 0.2% nitric acid and Cu was atomized at 2300°C using graphite furnace system and estimated at 324.8 nm using a hollow cathode lamp. Absorbance values were recorded thrice and the mean values were used for calculation[25].

LOX activity assay

LOX catalytic activity was measured based on the rate of deamination of 1,5-Diaminopentane (DAP) through detecting the amount of hydrogen peroxide (H_2O_2) released in the reaction. Liberated H_2O_2 oxidize amplex red into fluorescent resorufin at 1:1 ratio in the presence of enzyme hydrogen peroxidase. Assay protocol as follows, to 100 µL reaction mixture [0.15 M boric acid and 0.12 M sodium chloride pH 8.2, 50 µM N-acetyl-3,7-dihydroxyphenoxazine (Amplex Red, Molecular Probes, Invitrogen, USA), 0.1 Unit/mL horseradish peroxidase (HRP, Cat # P8375, Sigma) and 10 mM DAP (Cat # C8561, Sigma)], 100 ng of purified mLOX enzyme was added and the total reaction volume was 200 µL. All experiments were performed in opaque black 96 well microplate (Cat # 655076, Greiner bio-one) and the full protocol was carried out in dark environment, buffer and other constituents were prepared in double distilled water. The fluorescent end product was excited at 563 nm and the emission was read at 587 nm for 90 min with 5 min intermittent reading with a spectrophotometer (SpectramaxM2^e plate reader, Molecular Devices, USA). Sample lacking mLOX enzyme was used to collect the background readings and was used for calculating the enzyme activity. A linearity curve for standard hydrogen peroxide H_2O_2 (0-2000 nm) was plotted and the enzyme activity was calculated.

Determination of pH, temperature and substrate optima, enzyme kinetics and inhibitor studies of LOX

Purified mLOX enzyme (100 ng) was incubated with buffer systems with the pH range of 6-10: 0.1 M sodium phosphate buffer (0.1 M disodium

hydrogen phosphate with 0.1 M sodium dihydrogen phosphate,pH 6.5 and 7.5), 0.1 M borate buffer (0.1 M boric acid with 25 mM sodium tetraborate with 75 mM NaCl, pH 8 and 8.5) and 0.2 M glycine-NaOH buffer (pH 9, 9.5 and 10). Enzyme mLOX was pre-incubated in respective buffers for 30 min at 37°C and assay were performed.Well which received only reaction mixture without mLOX enzyme, incubated with respective buffer was used for background corrections. The optimum temperature for mLOX enzyme catalytic activity was determined by pre-incubating the enzyme at various temperatures (25°C, 37°C, 50°C and 75°C) with substrate DAP. Recombinant mLOX 100 ng was incubated with 100 mM of DAP for 15 min at designated temperatures then the reaction mixture was added and fluorescent reading was measured as endpoint. The total reaction volume was 200 µL. A blank sample (without mLOX) was included for respective temperatures and background corrections were made for each condition, respectively. Michaelis constant (K_m) value of the purified enzyme was estimated for DAP concentration range from 0.01-0.4M. Using the Lineweaver-Burk plots K_m, V_{max} and $k_{cat}$for mLOX were calculated. Homocysteine (Hcys) and βAPN were used for inhibitor studies. Recombinant mLOX enzyme (100 ng) was pre-incubated with various concentration of inhibitors at 37°C for 5 min and reaction mixture containing 100 mM of DAP was added and enzyme activity was measured.Interference from Hcys was accounted cautiously as it can react with amplex red directly. Here, a sample with only reaction mixture and Hcys without mLOX enzyme served as the blank and the readings were used for background corrections. Three independent experiments were performed and mean ± SD values were represented.

Immunofluorescence staining of collagen in ARPE 19 cells

Adult Retinal Pigment Epithelial (ARPE19) cells (ATCC-CRL-2302) (ATCC, USA) were cultured in DMEM-F12 (Sigma-Aldrich, USA), 14.2 mM sodium bicarbonate with 10% (*v/v*) fetal bovine serum at 37°C with 5% CO2. Cells were grown to 70-80% confluence and serum starved for overnight. It was then treated with various concentrations (1 to 1000 ng/mL) of recombinant mLOX for 72 h. TGF-β, known to induce collagen and LOX synthesis, was used as positive control at the concentration of 2.5 ng/mL. After treatment,cells were fixed with 4% formal dehydefor 10 min followed by permeabilization with 0.1% Triton-X for 5 min and blocked with 1% bovine serum albumin for 1 h. The cells were then incubated with anti-collagen primary antibody (Cat #PA1-36058, Thermo Fischer Scientific) at 1:100 dilution for overnight at 4°C followed by incubation with 1:700 diluted Alexa-488 conjugated anti-rabbit secondary antibody (Cat #A-11008, Invitrogen, Thermo Fischer Scientific). Images were taken using Axio Observer Z.1 microscope with a numerical aperture of 0.55 (Carl Zeiss, Gottingen, Germany). Axio Vision Rel. 4.8 software was used to analyze the images.

Circular dichroism

Circular Dichroism (CD) spectra of recombinant mLOX were collected using CD spectrometer (JASCO J-815, Tokyo, Japan) equipped with peltier temperature control. Throughout the experiment, nitrogen gas was blown into cuvette chamber to avoid any condensation. For all CD experiments, 1 mg/mL of mLOX and cuvette path length of 10 mM was used. CD spectrum was acquired in the far UV-region (200-240 nm)[26]. Secondary structure was predicted using the K2D2 software. For CD melting curve experiment,the ellipticity of mLOX at 208 and 222 nm was monitored. For the unfolding experiment, ellipticity was collected from 20-90°C with a step wise increment of 1°C. For refolding experiment, the temperature was decreased from 90-20°C with a decrement of 1°C. Ellipticity value for a buffer in the far UV-region was acquired and background correction was performed[27].

Intrinsic fluorescence of mLOX

Tryptophan residues in mLOX were excited at 295 nm and fluorescent emission spectra were recorded from 300 nm to 400 nm[28,29]. mLOX (3 µM) was suspended in 200 µL of 0.2 M glycine-NaOH buffer (pH 8.0) with 10% glycerol. For disulfide reduction, mLOX protein was treated with 100 mM DTT for 15 min at 60°C and then the spectrum was collected. For denaturation, mLOX was treated with 2M guanidine hydrochloride (GnHCl) for 15 min at 37°C and the spectrum was collected.The total reaction volume was 200 µL. Three independent experiments were performed and mean ± SD values were represented.

Extrinsic fluorescence analysis of mLOX

Binding of 8-Anilino-1-napthalenesulfonic acid (ANSA) to mLOX was studied by excitation at 370 nm and emission spectra were recorded from

400 to 600 nm[30]. mLOX (3 µM) was treated with ANSA in 1:100 ratio and incubated at 37°C for 30 min and the spectrum was obtained. Total reaction volume was 200 µL. Experiments were performed in triplicate and mean ± SD values were represented.

Results

Construction of pQE-30 XA + mLOX plasmid

PCR amplified mLOX product was inserted into the pQE-30 Xa plasmid and the plasmid was transformed into M15 (pREP4) *E. coli*. The plasmid was isolated from the positive clones and was confirmed by restriction digestion. Thus, the transformed M15 (pREP4) *E. coli* contained the complete pQE-30 Xa + mLOX construct (Fig. 1A). DNA sequencing confirmed that the inserted LOX sequence was free of any mutation.

Purification and confirmation of recombinant mLOX

Transformed bacterial cells upon induction with IPTG expressed mLOX, which was purified using Ni-NTA affinity column. Purified fraction showed a single band at 29 kDa (Fig. 1B), corresponding to the molecular weight of mLOX. The purification yield was about 15 mg/L of broth.Western blot analysis revealed a single band at 29 kDa when probed using both LOX and His tag as shown in our previous report[22], which confirms the purity of purified

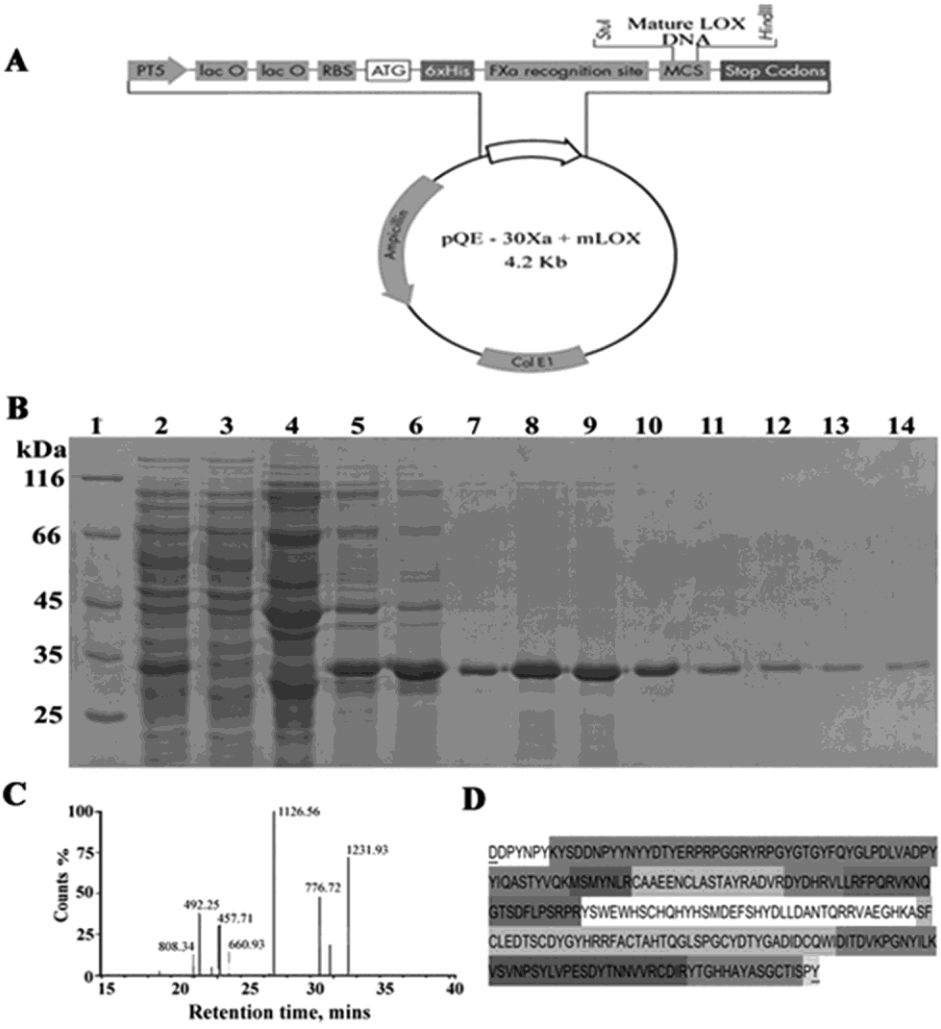

Fig. 1 — Plasmid construction, expression, purification and confirmation of mLOX. (A) pQE-30Xa+mLOX plasmid construct diagram (adapted and modified from Qiagen manual); (B) Silver-stained 10% SDS-PAGE gel showing the Ni-NTA affinity purification. Lane 1: Molecular size marker; Lane 2: Crude cell lysate; Lane 3: Ni-NTA unbound fraction; Lanes 4-6: fractions from 30 mM imidazole wash 1-3; Lanes 7-14: 250 mM imidazole eluted fraction from 2 to 8; (C) MS spectrum of a peptide derived from tryptic digestion of recombinant mLOX. The value on each peak denotes the m/z ratio of the peptide; and (D) Peptide map of mLOX identified by MS analysis. The intensity of the colour is based on the abundance of each peptide

recombinant mLOX. Mass spectrum of peptides derived from the purified recombinant mLOX (Fig. 1C) was analysed with PLGS, which showed a single hit for human LOX (UniProt ID p28300) with peptide coverage of 85% for mature LOX sequence. Peptides identified by MS analysis were within the mature LOX sequence (Fig. 1D), which indicates that recombinant mLOX preparation was pure.

Refolding of recombinant mLOX

In order to refold the purified mLOX, various buffers were screened (Table 1). Among them, glycine-NaOH buffer with 10% glycerol pH 8.0 showed no aggregation whereas rest of the screened buffers resulted in aggregation of recombinant mLOX. Recombinant mLOX was refolded by stepwise reduction in urea concentration by dialysis against this buffer. The dialysate was inspected for protein aggregates by centrifugation (10000 g for 30 min) at the end of each buffer change, which again revealed no aggregate in the glycine-NaOH buffered sample. Thus, the optimised buffer was used for further mLOX analysis. Using factor Xa endoprotease, His tag was cleaved from the refolded mLOX with 70% efficiency. Cleavage was confirmed by western blot analysis against LOX and His tag antibody, this data has been shown in our earlier report[22].

Estimation of copper in recombinant mLOX

From the standard copper concentration, it was calculated that 67 ± 2.8% of recombinant mLOX was found in the copper bound state.

Substrate specificity and effect of pH and temperature on recombinant mLOX activity

Enzymatic action of recombinant mLOX (100 ng) was tested against natural substrates; elastin, collagen and pseudo substrate DAP. With increasing concentration of DAP the enzymatic activity increased (10 mM: 1.15 ± 0.4 nmol of H_2O_2 released/min and 100 mM: 4.7 ± 0.4 nmol of H_2O_2 released/min) whereas, mLOX showed lesser activity against elastin and collagen (elastin 100 µg: 1.59 ± 0.7 nmol of H_2O_2 released/min and collagen 100 µg: 1.37 ± 0.4 nmol of H_2O_2 released/min) even at higher concentration (Fig. 2A). Recombinant mLOX was incubated with various buffer systems with pH ranging from of 6.5 to 10 and the enzymatic activity was evaluated. Optimal enzyme activity was found to be at the pH 8 (Fig. 2B). The catalytic activity was found to be decreased at acidic (<7) and more basic pH (>8.5) condition. Dependence of reaction-rate of mLOX on temperature was evaluated by assessing its activity under various temperatures (25°C, 37°C, 50°C and 75°C). Interestingly, the catalytic action of mLOX increased with increasing temperature (Fig. 2C). The temperature stability of mLOX was assessed from a structural aspect (CD spectra, intrinsic and extrinsic protein fluorescence) in the following sections.

Table 1 — Screening of various buffers for recombinant LOX solubility

Buffer	Visible aggregation Check	Centrifugation at 10000 rpm for 10 mins	Protein conc. in supernatant compared to the original conc.
HEPES-NaOH buffer	Aggregated	Pelleted	10%
Tris-HCl Buffer	Aggregated	Pelleted	1%
Potassium phosphate buffer	Aggregated	Pelleted	20%
Borax – Boric acid buffer	No aggregation	Small pellet	50%
Arginine- NaOH buffer,	Aggregated	Pelleted	10%
Glycine – NaOH buffer	No aggregation	No pellet	95%

Kinetics analysis of mLOX

Effect of varying DAP concentration on recombinant mLOX activity was evaluated. With the Lineweaver-Burk plot (Fig. 2D), K_m of recombinant mLOX for DAP was calculated to be 3.72×10^{-4} M, estimated V_{max} was 1.25 Units/mg of mLOX (Units = µmoles of $H_2O_2 s^{-1}$) and k_{cat} of $7.29 \times 10^3\ s^{-1}$. With this, we calculated the catalytic efficiency (k_{cat}/K_m) of mLOX and it was found to be $1.96 \times 10^7\ M^{-1} s^{-1}$.

The biological activity of recombinant mLOX

Collagen is one of the endogenous substrates for LOX and it augments the cross-linking of collagen. Staining of collagen in mLOX treated ARPE19 cells revealed long and thick bundles of collagen. Control cells (Fig. 3A) didn't show collagen fibre staining but cells treated with TGF-β (Fig. 3B) showed collagen fibre staining pattern and served as the positive control. When cells were treated with mLOX, collagen fibre staining increased with the increasing concentration of mLOX (Fig. 3C-F). The staining pattern of cells with 1000 ng/mL of mLOX (Fig. 3F) was comparable with TGF-β treated cells (Fig. 3B). Thus, recombinant mLOX was observed to be biologically active.

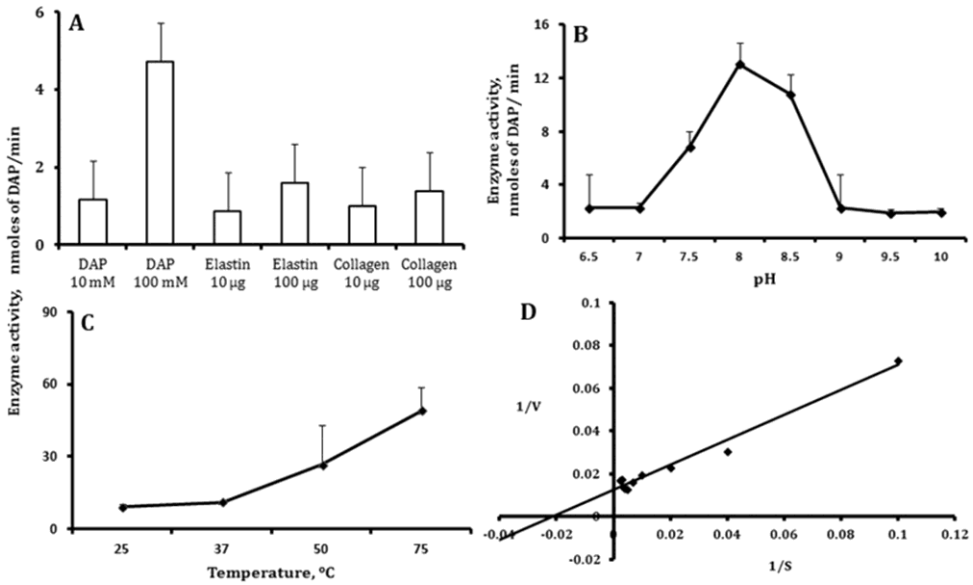

Fig. 2 — Enzymatic characterization of mLOX. Recombinant mLOX (100 ng) and reaction mixture were treated at respective conditions (as described in materials and methods) and readings were taken fluorometrically (Excitation 563 nm; Emission 587 nm). (A) Comparison of enzymatic activity of mLOX upon various substrates; (B) Effect of pH on recombinant mLOX activity; (C) Effect of temperature on recombinant mLOX activity; and (D) Lineweaver-Burk plot of recombinant mLOX for DAP substrate

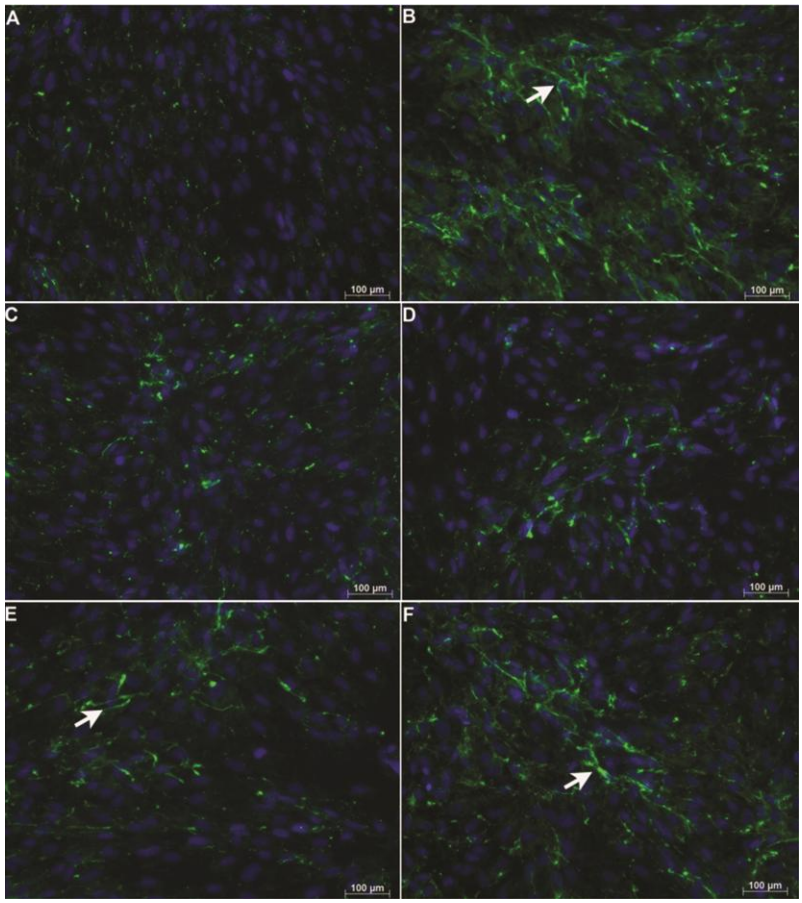

Fig. 3 — Biological activity of mLOX in ARPE-19 cells. (A) Cells received only basal media served as control; (B) Cells exposed to TGF-β (2.5 ng/mL) served as a positive control; and (C-F) Cells exposed to various concentrations of recombinant mLOX (1, 10, 100 & 1000 ng/mL). All images were acquired with 10X objective. Arrow indicates stained collagen fibres

Validation of inhibitors using recombinant mLOX

Enzymatic activity of the recombinant mLOX was assessed with inhibitors such as βAPN and Hcys by amplex red assay using DAP as substrate. Enzymatic activity of recombinant mLOX was inhibited up to 50% by Hcys at 30 μM concentration (Fig. 4A) whereas βAPN showed only 20% of enzyme inhibition at a much higher concentration of 400 μM (Fig. 4B). These results clearly indicate that Hcys inhibits mLOX better than βAPN.

Far UV-CD spectrum analysis of recombinant mLOX

The mLOX suspended in 0.2 M glycine-NaOH buffer (pH 8.0) with 10% glycerol showed α-helix of 8.43% and β-strand of 22% (Fig. 5A). Melting experiment of mLOX was performed using 50 mM glycine-NaOH buffer (pH 8.0) with 1.5% glycerol, to avoid interference. In the melting curve study, the degree of ellipicity at 222 nm and 208 nm was found to be unaltered in the unfolding (20-90°C) and refolding experiment (90-20°C) (Fig. 5B & C). This shows that mLOX maintains its secondary structure till 90°C and is resistant to higher temperature.

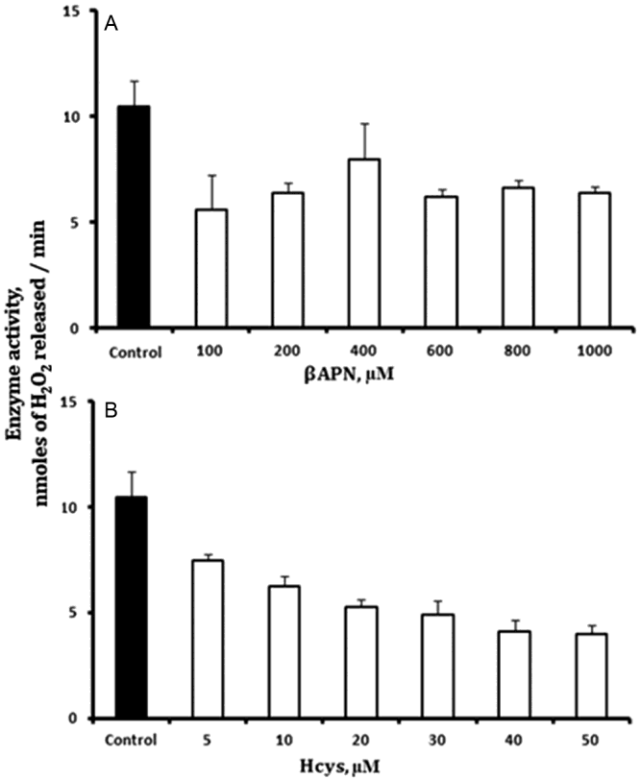

Fig. 4 — Enzyme activity of mLOX on DAP in the presence of inhibitors. (A) Inhibition of mLOX activity by βAPN; (B) Inhibition of mLOX activity by Hcys. One hundred nanograms of recombinant mLOXand 100 mM of DAP were pre-incubated at 37°C for 5 min with a respective concentration of inhibitors and reaction mixture was added and readings were taken fluorometrically (Excitation 563 nm; Emission 587 nm)

Tryptophan fluorescence emission of DTT-reduced recombinant mLOX

Recombinant mLOX gave heterogenous tryptophan emission peaks, one peak with the maximum quantum yield at 304 nm and another small peak at 333-335 nm.

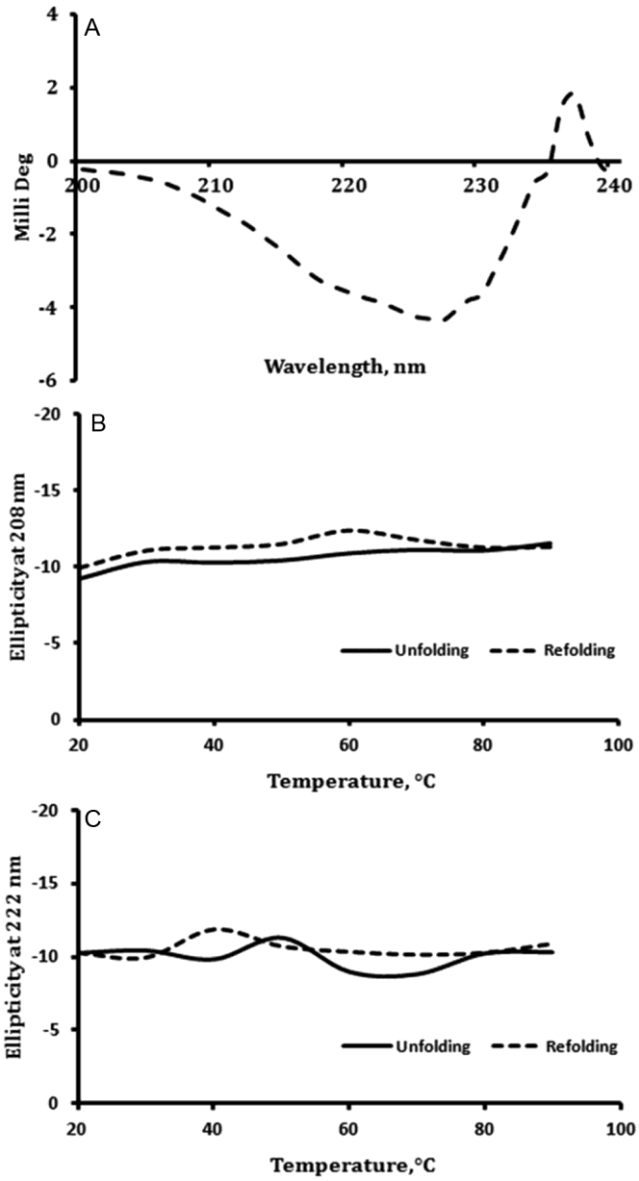

Fig. 5 — Far-UV CD spectrum of mLOX. Recombinant mLOX (1 mg/mL) was suspended in 200 mM glycine-NaOH buffer (pH 8.0) with 10% glycerol. (A) Spectrum was collected from 200 nm to 240 nm thrice and the cumulative average was taken finally; (B & C) CD melting curves, monitored ellipticity at 208 and 222 nm. The solid line represents unfolding condition (20 to 90°C) and dotted line represent refolding condition (90 to 20°C). mLOX was suspended in 50 mM glycine-sodium hydroxide buffer (pH 8.0) with 1.5% glycerol

Heterogenous peaks might be due to the localization of tryptophan at the varied environment. Upon reduction of disulfide bonds, emission peak at 304 nm showed a red shift to 308 nm and fluorescence intensity reduced with increasing DTT from 20 to 100 mM. The emission spectra at 333 nm was undisturbed upon reduction with DTT (Fig. 6A).

ANSA binding analysis of reduced and denatured recombinant mLOX

ANSA is a chemical molecule which binds to the exposed hydrophobic patches in a protein surface[30]. Recombinant mLOX showed an emission maximum at 450 nm. The DTT (100mM) reduced mLOX showed a red shift in the emission maxima from 450 to 470 nm, which shows the unfolding of the recombinant mLOX. Recombinant mLOX denatured with 2M GnHCl did not show much change in the emission spectra. When recombinant mLOX was reduced with DTT (100 mM) and denatured with GnHCl (2 M) the emission spectra showed a shift in the emission maxima to 470 nm and an increase in the fluorescence value from 250 RFU to 400 RFU. This shows that unfolding leads to exposure of a more hydrophobic region of the mLOX, which resulted in increased binding of ANSA (Fig. 6B).

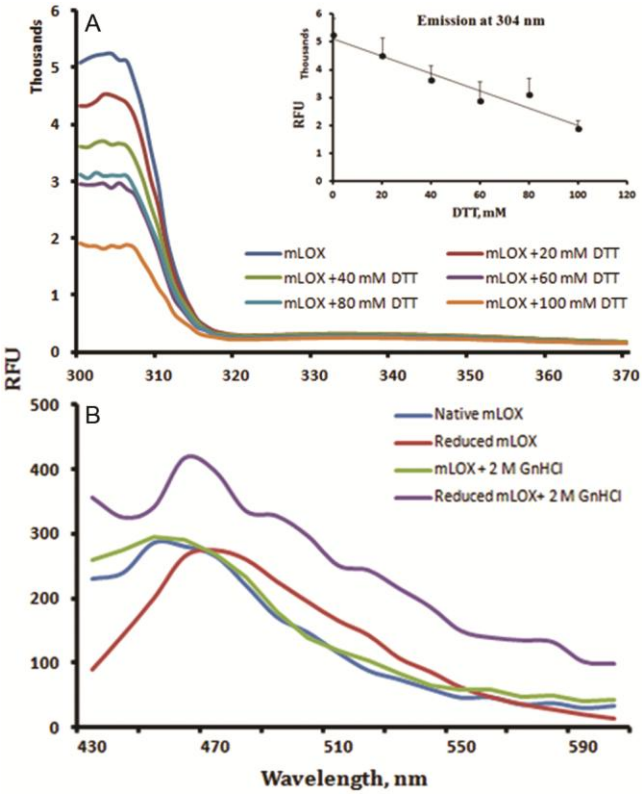

Fig. 6 — Intrinsic and extrinsic fluorescence of mLOX. (A) Tryptophan fluorescence emission spectrum of native and reduced recombinant mLOX. Recombinant mLOX (3 μM) was reduced with different concentrations of DTT (20-100 mM) at 60°C. Intrinsic fluorescence of mLOX was measured by exciting at the wavelength of 295 nm and emission spectrum was collected from 300 to 370 nm with an interval of 1 nm. Inlet showing the emission at 304 nm of mLOX treated with a varing concentration of DTT; (B) ANSA binding - Extrinsic fluorescence of recombinant mLOX. Recombinant mLOX(3 μM)was reduced with 50 mM DTT at 60°C and denatured with 2 M GnHCl and then exposed to ANSA in 1:100 ratio of protein concentration. ANSA binding was assessed by exciting at 370 nm and emission spectrum was collected from 400-600 nm. Data shown represent mean from three independent experiments. (RFU –Relative Fluorescence Unit).

Discussion

We report the characterization of recombinant mLOX using a glycine-NaOH buffer which maintains mLOX in its solubilised form even without urea. Here we demonstrated that purified mLOX is biologically active and thermally stable. Thermo-stability of mLOX is attributed to its disulfide linkage.

Recombinant mLOX has been purified using infusion cloning method. Purification yield was up to 15 mg/L of LB broth, which was higher than the earlier reports[31,32]. Characterization of LOX is challenging because of the non-availability of buffers that would maintain LOX in its solubilised state. An earlier report[31] indicated solubility of LOX in 10 mM potassium phosphate buffer but in the present study, mLOX got precipitated in the same. Therefore, it was necessary to screen various buffers which maintain the protein without aggregation. Among the various buffers screened, the glycine-NaOH buffer with 10% glycerol pH 8.0 was identified as an ideal buffer. Presence of glycine and glycerol would have maintained the enzyme in a solubilised state. Glycine acts as a protein stabilizing agent by preferential exclusion mechanism and thereby reducing the surface tension[33]. Glycerol is reported to enhance the thermodynamic stabilization of protein[34] and pushes the hydrophobic region of a protein inside and thereby preventing inter-molecular interaction[35,36]. Probably, synergistic action of glycine and glycerol has maintained the solubility of mLOX in a solution state.

Recombinant mLOX contains His tag in its N-terminal. Histidine residues have an affinity for copper, which might interfere with the activity of copper-dependent LOX. Hence, His tag was removed using endoprotease factor Xa and ascertained the activity of recombinant mLOX. Previous reports[31,32,37] which demonstrated the activity of LOX had retained the His tag. Hence, this is the first report where

mLOX has been characterized without the presence of fusion tags.

In our study, the pseudosubstrate DAP showed maximal activity when compared to the natural substrates. This might be due to the non-availablity of free peptidyl lysine in elastin and collagen. Our results also indicated that the recombinant mLOX showed maximum activity at pH 8.0. (Fig. 2B) which was in accordance with an earlier report on LOX, purified from the *Dosidicus gigas*, which had maximum activity between the pH 8 to 8.2[38]. It was reported that LOX oxidises basic globular proteins with a pI value of > 8.0 and not the neutral and acidic proteins[39].

Recombinant mLOX, showed maximal enzyme activity V_{max} to be 1.25 Unit/mg (Units = µmoles of $H_2O_2s^{-1}$), which was higher than the previous reports. Herwald *et al.* showed 0.31 Unit/mg (1 Unit = 1 nM of DAP/min) of recombinant LOX activity using amplex red assay[32]. whereas, Jung *et al.* purified LOX by cloning and showed activity of 0.097 Unit/mg (1 Unit = 1 µM of benzyl amine/min) using amine oxidase activity assay[31]. However, recombinant mLOX showed low affinity against the DAP (K_m 3.72 × 10^{-4} M). whereas, Palamkumbura *et al.* determined K_m for LOX towards DAP to be 0.5 mM[40]. The possible reason for this difference may be due to the variation in enzyme sources where the present study used purified recombinant human mLOX, while the earlier study used LOX that was purified from bovine aorta.

Immunofluorescence staining of collagen fibres in ARPE-19 cellsshowed increased collagen cross-linking in dose-dependent manner to exogenously added recombinant mLOX (Fig. 3C-F). Earlier Kothapalli *et al.*[41] and Markris *et al.*[42] reported exogenous addition of LOX increases cross-linking of elastin and collagen, respectively. The enhanced collagen bundles confer that recombinant mLOX is biologically active. Since recombinant mLOX is biologically active, it would be suitable for angiogenesis and other *in vitro* assays.

Secondary structure analysis of mLOX by CD spectra indicated that the degree of secondary structure of the refolded mLOX (α-helix of 8.43% and β-strand of 22%) was in accordance with the secondary structure of our reported mLOX model (13.5% of α-Helix and 16.4% of β-Sheet)[21]. Our previously reported LOX model has a higher affinity for Hcys (−9.53 kcal/ mol) than the established inhibit or βAPN (−6.29 kcal/mol). Further, we discussed the nature of the catalytic cavity of LOX and its interacting residues with the substrate and inhibitors[21]. The present study shows that Hcys inhibits mLOX activity even at a lower concentration of 30 µM than βAPN, which inhibits LOX at 400 µM. Thus, the secondary structure of refolded mLOX and the outcome of the inhibitor assay in the present study correlates with our reported *in silico* results.

In the current study, enzymatic action of mLOX was observed even at 75°C which was in agreement with a study by Torres-Arreola *et al.* which showed LOX activity of *Dosidicus gigas* up to 70°C[38]. Correspondingly, the secondary structure of mLOX was found to be stable till 90°C as observed in the melting experiments using CD spectra (Fig. 5B & C). Hence, thermo-stable nature of LOX has been experimentally proved here.

Chen *et al.* stated that disulfide bonds in LOX render rigidity and high resistance to denaturants[37]. To examine the rigid nature of LOX, we studied the intrinsic and extrinsic fluorescence of mLOX under native and disulfide reduced conditions. mLOX has 3 tryptophan residues (at 286, 288 and 363 positions) among them 286th and 288th residues are present in the buried conserved copper-binding site. Tryptophan emission of mLOX resulted in heterogeneous emission with a major and minor fluorescence at 304 nm and 333 nm respectively, (Fig. 6A). Heterogeneous emission arises when tryptophan residues in a protein are present in both buried and exposed region. On reduction of disulfide bonds in mLOX, tryptophan emission spectra showed a red shift in the lambda max from 304 to 307 nm with a fall in the quantum yield from 5000 RFU to 2000 RFU (Fig. 6A). The red shift shows the unfolding and fall in quantum yield is due to the exposure of buried tryptophan residues. No significant change was observed with the minor peak at 333 nm. Hence, refolded mLOX possess tryptophan in its core as well as in surface of its structure. Our *in silico* report[21] on LOX structure show tryptophan *i.e.* 286th and 288th residues present in the buried region along with copper binding site and 363rd tryptophan residue present at the exposed region. Similarly, ANSA exhibits higher fluorescence intensity when disulfide bonds are reduced compared to the native mLOX. Reduction of disulfide bond also favours the unfolding action of GnHCl. Hence, intrinsic and

extrinsic fluorescence experiments explain that disulfide bonds hold the structure and render resistance for LOX against temperature and denaturant. Similarly, Jana *et al.* demonstrated that the structure of streptomycin adenyl transferase is stabilized by disulfide bonds using tryptophan emission and ANSA binding analysis[43]. To the best of our knowledge, this is the first study on tryptophan localisation of LOX in its structure and explains disulfide bond involvement in the stability of LOX structure.

In summary, the present work reports a buffer to maintain native mLOX enzyme in aqueous buffer without any aggregation. This buffer can facilitate elucidation of the crystal structure of LOX through crystallography studies. Intrinsic and extrinsic fluorescence data explains the stability of LOX under unusual conditions. Further, the biologically active mLOX can be utilized to understand the disease mechanism where LOX is implicated.

Acknowlegdment

Authors thank the Indian Council of Medical Research (ICMR) for providing the grant (Project No.52/6/2009-BMS). We thank Department of Biotechnology, Indian Institue of Technology Madras, for permitting to utilize their CD spectroscopy facility.

References

1 Trackman PC, Bedell-Hogan D, Tang J & Kagan HM, Post-translational glycosylation and proteolytic processing of a lysyl oxidase precursor. *J Biol Chem*, 267 (1992) 8666.

2 Siegel RC, Pinnell SR & Martin GR, Cross-linking of collagen and elastin. Properties of lysyl oxidase. *Biochemistry*, 9 (1970) 4486.

3 Barker HE, Cox TR & Erler JT, The rationale for targeting the LOX family in cancer. *Nat Rev Cancer*,12 (2012) 540.

4 Postovit LM, Abbott DE, Payne SL, Wheaton WW, Margaryan NV & Sullivan R, Hypoxia/reoxygenation: a dynamic regulator of lysyl oxidase-facilitated breast cancer migration. *J Cell Biochem*, 103 (2008) 1369.

5 Cox TR, Bird D, Baker AM, Barker HE, Ho MWY & Lang G, LOX-mediated collagen crosslinking is responsible for fibrosis-enhanced metastasis. *Cancer Res*, 73 (2013) 1721.

6 Canesin G, Cuevas EP, Santos V, López-Menéndez C, Moreno-Bueno G & Huang Y, Lysyl oxidase-like 2 (LOXL2) and E47 EMT factor: novel partners in E-cadherin repression and early metastasis colonization. *Oncogene*, 34 (2015) 951

7 Osawa T, Ohga N, Akiyama K, Hida Y, Kitayama K, Kawamoto T, Yamamoto K, Maishi N, Kondoh M, Onodera Y, Fujie M, Shinohara N, Nonomura K, Shindoh M & Hida K, Lysyl oxidase secreted by tumour endothelial cells promotes angiogenesis and metastasis. *Br J Cancer*, 109 (2013) 2237.

8 Baker AM, Bird D, Welti JC, Gourlaouen M, Lang G, Murray GI, Reynolds AR, Cox TR & Erler JT, Lysyl oxidase plays a critical role in endothelial cell stimulation to drive tumor angiogenesis. *Cancer Res*, 73 (2013) 583.

9 Bais MV, Nugent M, Stephens DN, Sume SS, Kirsch KH, Sonenshein GE & Trackman PC, Recombinant lysyl oxidase propeptide protein inhibits growth and promotes apoptosis of pre-existing murine breast cancer xenografts. *PLoS One*, 7 (2012) e31188.

10 Min C, Kirsch KH, Zhao Y, Jeay S, Palamakumbura AH, Trackman PC & Sonenshein GE, The tumor suppressor activity of the lysyl oxidase propeptide reverses the invasive phenotype of Her-2/neu-driven breast cancer. *Cancer Res*, 67 (2007) 1105.

11 Nareshkumar RN, Sulochana KN & Coral K, Inhibition of angiogenesis in endothelial cells by human lysyl oxidase propeptide. *Sci Rep*, 8 (2018) 10426.

12 Kasashima H, Yashiro M, Kinoshita H, Fukuoka T, Morisaki T, Masuda G, Sakurai K, Kubo N, Ohira M & Hirakawa K, Lysyl oxidase is associated with the epithelial-mesenchymal transition of gastric cancer cells in hypoxia. *Gastric Cancer*, 19 (2016) 431.

13 Cheon DJ & Orsulic S, Ten-gene biomarker panel: a new hope for ovarian cancer? *Biomark Med*, 8 (2014) 523.

14 Mesarwi OA, Shin MK, Drager LF, Bevans-Fonti S, Jun JC, Putcha N, Torbenson MS, Pedrosa RP, Lorenzi-Filho G, Steele KE, Schweitzer MA, Magnuson TH, Lidor AO, Schwartz AR & Polotsky VY, Lysyl oxidase as a serum biomarker of liver fibrosis in patients with severe obesity and obstructive sleep apnea. *Sleep*, 38 (2015) 1583.

15 Wang J, Zhu Y, Tan J, Meng X, Xie H & Wang R, Lysyl oxidase promotes epithelial-to-mesenchymal transition during paraquat-induced pulmonary fibrosis. *Mol Biosyst*, 12 (2016) 499.

16 Wordinger RJ & Clark AF, Lysyl Oxidases in the trabecular meshwork. *J Glaucoma*, 23 (2014) S55.

17 Park HYL, Kim JH & Park C K, Lysyl oxidase-like 2 level and glaucoma surgical outcomes. *Invest Opthalmol Vis Sci*, 55 (2014) 3337.

18 Eliades A, Papadantonakis N, Bhupatiraju A, Burridge KA, Johnston-Cox HA, Migliaccio AR, Crispino JD, Lucero HA, Trackman PC & Ravid K, Control of megakaryocyte expansion and bone marrow fibrosis by lysyl oxidase. *J Biol Chem*, 286 (2011) 27630.

19 Rodriguez-Pascual F & Rosell-Garcia T, Lysyl oxidases:functions and disorders. *J Glaucoma*, 27 (2018) S15.

20 Rodríguez C, Martínez-González J, Raposo B, Alcudia JF, Guadall A & Badimon L, Regulation of lysyl oxidase in vascular cells: Lysyl oxidase as a new player in cardiovascular diseases. *Cardiovasc Res*, 79 (2008) 7.

21 Bhuvanasundar R, John A, Sulochana KN, Coral K, Deepa PR & Umashankar V, A molecular model of human Lysyl Oxidase (LOX) with optimal copper orientation in the catalytic cavity for induced fit docking studies with potential modulators. *Bioinformation*, 10 (2014) 406.

22 Mohankumar A, Renganathan B, Karunakaran C, Chidambaram S & Natarajan SK, Peptides derived from the copper-binding region of lysyl oxidase exhibit antiangiogeneic properties by inhibiting enzyme activity: an *in vitro* study. *J Pept Sci*, 20 (2014) 837.

23 Gosavi RA, Mueser TC & Schall CA, Optimization of buffer solutions for protein crystallization. *Acta Crystallogr D Biol Crystallogr*, 64 (2008) 506.

24 Tsumoto K, Ejima D, Kumagai I & Arakawa T, Practical considerations in refolding proteins from inclusion bodies. *Protein Expr Purif*, 28 (2003) 1.

25 Narayanan G, Bharathidevi SR, Vuyyuru H, Muthuvel B & Konerirajapuram NS, CTR1 Silencing Inhibits Angiogenesis by Limiting Copper Entry into Endothelial Cells. *PLoS One*, 8 (2013) e71982.

26 Das N, Maity S, Chakraborty J, Pal S, Sardar S & Halder UC, Purification and characterization of a gelatinolytic serine protease from the seeds of ash gourd *Benincasa hispida* (Thunb.) Cogn. *Indian J Biochem Biophys*, 55 (2018) 77.

27 Greenfield NJ, Using circular dichroism spectra to estimate protein secondary structure. *Nat Protoc*, 1 (2007) 2876.

28 Chen Y & Barkley MD, Toward understanding tryptophan fluorescence in proteins. *Biochemistry*, 37 (1998) 9976.

29 Chilom C & Nistorescu A, A spectroscopic study of the interaction of HSA with tetracaine. *Indian J Biochem Biophys*, 53 (2016) 206.

30 Matulis D, Baumann CG, Bloomfield VA & Lovrien RE, 1-anilino-8-naphthalene sulfonate as a protein conformational tightening agent. *Biopolymers*, 49 (1999) 451.

31 Jung ST, Kim MS, Seo JY, Kim HC & Kim Y, Purification of enzymatically active human lysyl oxidase and lysyl oxidase-like protein from Escherichia coli inclusion bodies. *Protein Expr Purif*, 31 (2003) 240.

32 Herwald SE, Greenaway FT & Lopez KM, Purification of high yields of catalytically active lysyl oxidase directly from Escherichia coli cell culture. *Protein Expr Purif*, 74 (2010) 116.

33 Pikal-Cleland KA, Cleland JL, Anchordoquy TJ & Carpenter JF, Effect of glycine on pH changes and protein stability during freeze-thawing in phosphate buffer systems. *J Pharm Sci*, 91 (2002) 1969.

34 Rashid F, Sharma S, Baig MA & Bano B, Effect of polyols and salts on the acid-induced state of human placental cystatin. *Biochemistry* (*Mosc*), 71 (2006) 619.

35 Rariy RV & Klibanov M, Correct protein folding in glycerol. *Proc Natl Acad Sci U S A*, 94 (1997) 13520.

36 Sousa R, Use of glycerol, polyols and other protein structure stabilizing agents in protein crystallization. *Acta Crystallogr D Biol Crystallogr*, 51 (1995) 271.

37 Chen X & Greenaway FT, Identification of the disulfide bonds of lysyl oxidase.*J Neural Transm*(*Vienna*), 118 (2011) 1111.

38 Torres-Arreola W, Ezquerra-Brauer JM, Figueroa-Soto CG, Valenzuela-Soto EM, Garcia-Sanchez G, Marquez-Rios E & Pacheco-Aguilar R, Lysyl oxidase from jumbo squid (*Dosidicus gigas*) muscle: detection and partial purification. *Int J Food Sci Technol*, 46 (2011) 1711.

39 Kagan HM, Williams MA, Williamson PR& Anderson JM, Influence of sequence and charge on the specificity of lysyl oxidase toward protein and synthetic peptide substrates. *J Biol Chem*, 259 (1984) 11203.

40 Palamakumbura AH & Trackman PC, A fluorometric assay for detection of lysyl oxidase enzyme activity in biological samples. *Anal Biochem*, 300 (2002) 245.

41 Kothapalli CR & Ramamurthi A, Lysyl oxidase enhances elastin synthesis and matrix formation by vascular smooth muscle cells. *J Tissue Eng Regen Med*, 3 (2009) 655.

42 Makris EA, Responte DJ, Paschos NK, Hu JC & Athanasiou KA, Developing functional musculoskeletal tissues through hypoxia and lysyl oxidase-induced collagen cross-linking. *Proc Natl Acad Sci U S A*, 111 (2014) E4832.

43 Jana S, Chaudhuri TK & Deb JK, Effects of guanidine hydrochloride on the conformation and enzyme activity of streptomycin adenylyltransferase monitored by circular dichroism and fluorescence spectroscopy. *Biochem* (*Mosc*), 71 (2006) 1230.